International Journal of Engineering and Advanced Technology (IJEAT)
ISSN: 2249-8958 (Online), Volume-10 Issue-2, December 2020

Development of Soft-Switching PWM Full Bridge DC–DC Converter with Charging Applications

Meenavalli Harikrishna, Madugula Satya Harish, M.Veera ChandraKumar

Abstract*: This paper proposes a high-frequency-link soft switching pulse-width dc–dc converter for battery chargers. Zero-voltage switching of power switches is achieved from light load to full load. Reverse recovery losses can be reduced in the secondary side output diodes without using any additional circuit components. Zero-current switching of output diodes is achieved by using the series-resonant circuit in the secondary side .The circulating current in the primary side full-bridge circuit can be changed by the operation modes of the output diode current. As a result, a high efficiency can be achieved for EV on-board battery chargers. The performance of the proposed converter is evaluated throughout Matlab Simulation results for a 2.0-kW circuit

Keywords* : DC–DC Converter, High Frequency Link, Battery Charger

I. INTRODUCTION

As generally recognised electric vehicles can achieve higher energy conversion efficiency, motor-regenerative braking capability, fewer local exhaust emissions, and less acoustic noise and vibration, as compared to gas-engine vehicles. The battery has an important role in the development of electric vehicles (EVs) and plug-in hybrid electric vehicles (PHEVs).

Fig.1 Electric vehicle and its main modules

An EV shown in Fig..1 [1] is a vehicle propelled by electricity, unlike the conventional vehicles on road today which are major consumers of fossil fuels. This electricity can be either produced outside the vehicle and stored in a battery or produced on board with the help of fuel cells (FC's). The development of EV's started as early as1834 when the first batterypowered EV (tricycle) wasbuilt by Thomas Davenport [2],which appeared to be appalling, as it even preceded the invention of the ICE based on gasoline or diesel fuel. The development of EV's was discontinued as they were not very convenient and efficient to use as they were very heavy and took a long time to recharge .Moreover, from the end of the year 1910, they also became more expensive than ICE vehicles .This led to the development of gasolinebased vehicles However, there are concerns over the depletion of fossil fuel and green house gases causing long term global crisis like climatic changes and global warming. These concerns are shifting the focus back to development of automotive vehicles which use alternative fuels for operations .The development of such vehicles has become imperative not only for the scientists but also for the governments around the globe as can be substantiated by the Kyoto Protocol which has a total of 183 countries ratifying it (As on January 2009). The BEV has been since few years a very attractive research area both by car manufacturers and scientific researchers. The system architecture of HEV/EV

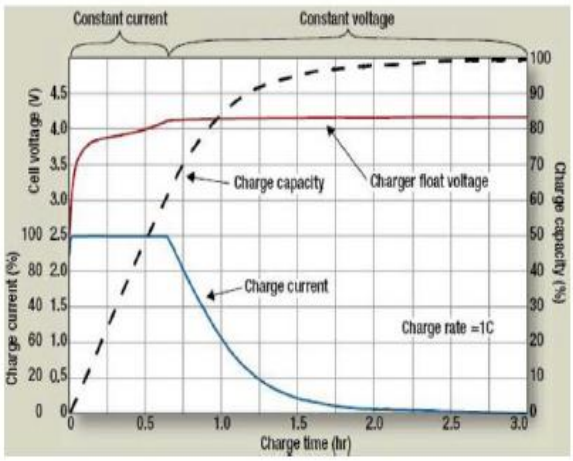

Fig. 2 Typical charging profile of Li-Ion cel

B. Charger Classifications

Since theinception of thefirst EVs,there havebeen many diff erent charging systems proposed. Due to many different configuration so fthechargers, itisrequired to classify them based on some common design and application features.Tab le1.1 [6] lists fivedifferent methods of classifying chargers

Battery charger classification

Revised Manuscript Received on December 25, 2020.
* Correspondence Author
Mr.Meenavalli Harikrishna*, Department of Electrical and Electronics Engineering, Pragati Engineering College, Surampalem, Peddapuram
Mr.Madugula Satya Harish, Department of Electrical and Electronics Engineering, Pragati Engineering College, Surampalem, Peddapuram
Mr. M. V. Chandra Kumar, Department of Electrical and Electronics Engineering, Pragati Engineering College, Surampalem

CLASSIFICATION TYPE	OPTIONAL
TOPOLOGY	DEDICTED,INTIGRATED
LOCATION	ON BOARD,OFF BOARD
CONNECTION TYPE	CONDUCTIVE,INDUCTIVE,MECHANICAL
ELECTRICAL WAVEFORMS	AC,DC
POWER LEVEL	LEVEL1,LEVEL2,LEVEL3

The chargers can be classified based on the circuit topologies [7]. A dedicated circuit solely operates to charge the battery. In comparison, the traction inverter drive can serve as the charger at the same time when the vehicle is not working and plugged into the grid for charging. This option is commonly known as integral/integrated chargers .A second classification is the location of the charger. Carrying the charger on-board greatly increases the charging availability of the vehicle. Off-board chargers can make use of higher amperage circuits and can charge a vehicle in a considerably shorter amount of time.

A.**Typical Battery Charging Profile**

A battery is a device whichconverts chemical energy directly into electricity It is an electrochemical galvanic cell or a combination of such cells which is capable of storing chemicalenergy. Batteries aremore desirable for the use invehicles, and particular traction batteries are most commonlyusedbyEVmanufacturers.Traction batteriesinclude LeadAcid type, Nickel and Cadmium, Lithium ion/polymer, So dium and Nickel

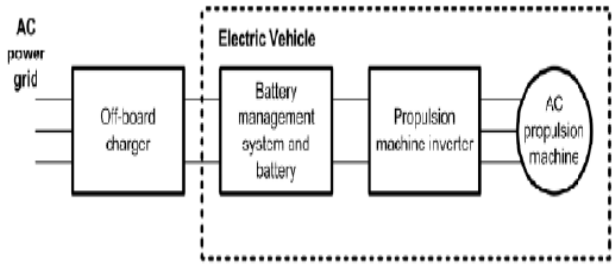

Fig.3 Block diagram of off-board charger

For off-board charger shown in Fig.3 [7], the charger is an external unit, rather than a component of the EV. Furthermore an off-board charger produces a high DC voltage .The internal battery management system (BMS) must be able to charge the battery using charge voltage. the major drawback of this topology is that the charger is not integrated in the EV.hence it is impossible to charge the battery of an EV with out an appoprivate charger which provides the needed high DC voltage on site.

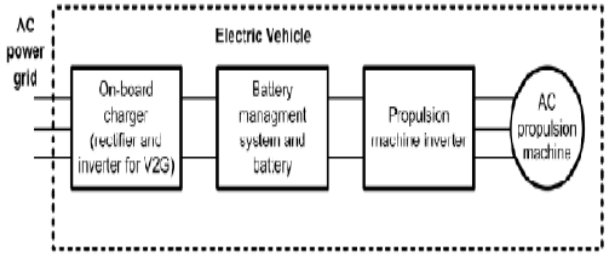

Fig.4 Block diagram of on-board charger

For on board charger shown in Fig 4 (7) The charger is a component of the EV.The EV can be charged almost every where using a single phase or three phase supply.The major drawback of this topology is that this simple on board charger requires an additions DC/AC inverter.One inverter enable the vahicle to grid (V2G) capability and the second drives the AC propulsion machine.Third is the connection method [8] conductive charging contains metal to metal contact inductive charging contacts ac grid to vehicle indirectly via a take a part high frequancy transformer and mechanical charging the depleted battery pack with a Full one in battery swap stations Fourth the electrical waveform aty the connection port of the vehicle to the grid can be either a dc connection or an ac connection currently the PHEVs and EVs in the market employ an ac connection type. However in the future the availability and commonality of the dc sources may change the connection type fifth the charger can deliver power in unidirection way by just charging the battery more advanced designs introduce bidirectional power transfer again alloff the chargers in the market employ unidirectional chargers.Last three charging levels have been defined forEVs and PHEVs. These are detailed in Table 3.2 Level 1 and level2 charging are assumed to be te normal charging levels which will take place where the vehicle will sit for a substantial amount of time such as the home or office. Howeverthe drawback of charging a vehicle with these normal charging levels is that is can take 4 to 20 hours depending on available power battery size and SOC of the battery and this is not a viable option when long travel distances are considered The solution to this lengthy charging time issue is the level 3 fast charging.level 3charging makes battery powered vehicle more competitive adainst conventional ICE vehicle by charging the battery in less than 30 minutes. typically level 3 charging is accomplished via an off board charger by means of converting three phase 480v AC to a regulated DC. Although there have not been any adopted standards for level 3charging in the US or internally other than japan .a japanese protocal known as CHADEMO is gaining international recognition CHAdeMO supplies the vehicle with a regulated DC voltage requiring an external charging station ,and interfaces directly with the vehicle battery and battery management system (BMS).

Alternatively, several European automakers are focusing on supplying vehicles directly with 3-phase and processing it via an on-board battery charger [17].

II. PRTOPOSED CONVERTER

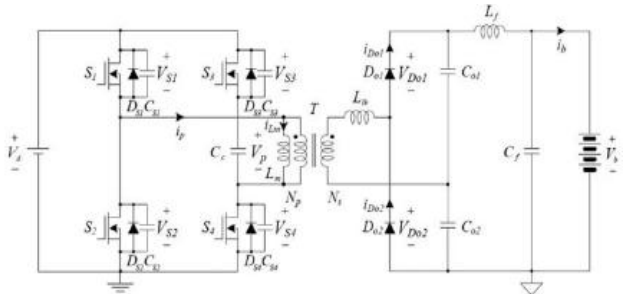

Fig.5. Circuit diagram of the proposed dc–dc converter.

Fig5 shows the circuit diagram of the proposed converter. The primary side circuit consists of power switches (S1, S2, S3, and S4), clamping capacitor (Cc), and transformer (T). Power switches are considered ideal switches except body diodes DS1–DS4 and output capacitors CS1–CS4. The transformer T has the magnetizing inductor Lm and leakage inductor Llk with the turns ratio of 1:N where N = Ns /Np . The secondary side circuit consists of the rectifier circuit (Do1, Do2, Llk, Co1, and Co2) and output filter (Lf , Cf). A series resonance between Llk, Co1 , and Co2 makes the output diodes to be turned ON and OFF at zero current. Vd is the input voltage of the proposed converter, which is generated by the front-end PFC converter. Vb is the battery voltage. Because the output filter has small values, the voltage Vt across the secondary side circuit is considered to be Vb for one switching period Ts (=1/fs).Fig. 4 shows the switching waveforms of the proposed converter for Ts . S1 (S2) and S4 (S3) are turned ON and OFF, simultaneously. S1 (S3) and S2 (S4) operate complementarily with a short dead time. The converter has six switching modes.

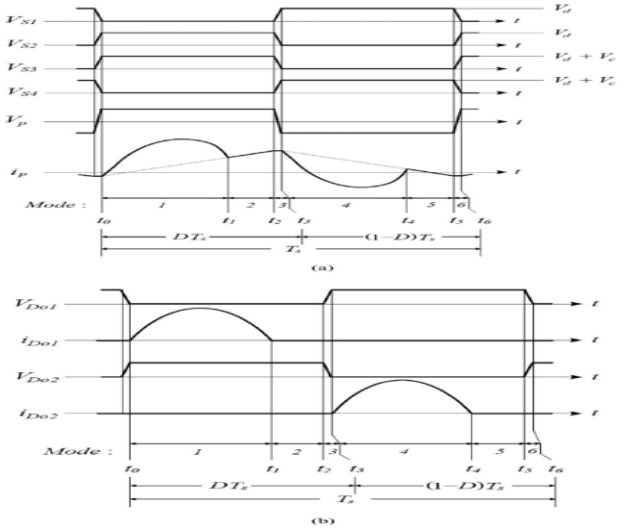

Fig.6. Switching waveforms of the proposed converter for Ts . (a)Wave forms of the primary side circuit. (b) Waveforms of the secondary side circuit .during Ts.

The duty ratio D is based on the on-time of S1 and S4. Then, the duty ratio of S2 and S3 is 1–D. Before t = t0, S2 andS3 have been turned OFF. The voltages VS1 and VS4 have been zero when the primary current ip flows through body diodes DS1 and DS4.

Mode 1 [t0 , t1]: At t = t0, S1 and S4 are turned ON at zero voltage. Since the voltage across Lm is Vd, the magnetizing inductor current iLm increases linearly as follows:

At ithe isecondary iside, iNVd iis iapplied ito ithe isecondary iwinding iof iT. iWhen ithe ioutput idiode iDo1 iis iturned iON, ia iseries iresonance ibetween iLlk, iCo1 i, iand iCo2 ioccurs. iThe ioutput idiode icurrent iiDo1 iis iexpressed ias ifollows: i

$$i_{Do1}(t) = \frac{V_b - NV_d - V_{Co1}}{Z_r\sqrt{L_{lk}/2C_r}} \sin\omega_r (t - t_0)$$

where VCo1 is the voltage across Co1 . ωr is the angular resonant frequency as follows:

$$\omega_r = 2\pi f_r = \frac{1}{\sqrt{2L_{lk}C_r}}.$$

Here, Cr is the capacitor as Cr = Co1 = Co2. Then, the primary current ip is expressed as follows:

$$i_p(t) = i_p(t_0) + \frac{V_d}{L_m}(t - t_0) + Ni_{Do1}(t).$$

Mode 2 [t1 , t2]: At t = t1 , the half-resonant period of iDo1is finished. iDo1 is zero before Do1 is turned OFF. Do1 can be turned OFF at zero current without any voltage overshoots and oscillations.

Mode 3 [t2 , t3]: At t = t2, S1 and S4 are turned OFF. The primary current ip charges CS1 and CS4 and discharges CS2 and CS3. VS1 increases from zero to Vd while VS4 increases from zero to Vd + Vc . VS3 decreases from Vd + Vc to zero while VS2 decreases from Vd to zero. Since the switch output capacitor CS(=CS1 = CS2 = CS3 = CS4) is very small, the time interval during this mode is considered negligible compared to Ts.

Mode 4 [t3 , t4]: At t = t3, S2 and S3 are turned ON at zero voltage. Since the voltage across Lm is −(Vd − Vc), the magnetizing inductor current iLm decreases linearly as follows:

$$i_{Lm}(t) = i_{Lm}(t_3) - \frac{(V_d - V_c)}{L_m}(t - t_3).$$

At the secondary side, N(Vd − Vc) is reversely applied across the secondary winding of T. When the output diode Do2 is turned ON, a series resonance between Llk, Co1, and Co2 occurs .The output diode current iDo2 is expressed as follows:

$$i_{Do2}(t) = \frac{N(V_d - V_c) + V_{Co2}}{Z_r}\sin\omega_r(t - t_3)$$

Published By:
Blue Eyes Intelligence Engineering
and Sciences Publication

$$i_p(t) = i_p(t_3) - \frac{(V_d - V_c)}{L_m}(t - t_3) - N i_{Do2}(t).$$

where VCo2 is the voltage across Co2 . The primary current ip is expressed as follows: according to different input voltage conditions and CS4 . VS1 decreases from Vd to zero while VS4 decreases from Vd + Vc to zero. VS3 increases from zero to Vd + Vc while VS2 increases from zero to Vd . The next switching cycle begins when S1 and S4 are turned ON at zero voltage again.

III. CONVERTER FEATURES

A. ZVS Condition

By the voltage–second balance relation on Lm during Ts, the voltage Vc is expressed as follows:

$$V_c = \frac{2D - 1}{1 - D} V_d.$$

For the voltage–second balance relation on the secondary winding of T during Ts , the following relation between Vd and Vb is obtained as follows:

$$\frac{V_b}{V_d} = \frac{N}{1 - D}.$$

The EV on-board battery charger commonly has a PFC converter and a high-frequency-link dc–dc converter. The PFC converter typically generates a high dc-link voltage around 380–400 V for the input voltage of the dc–dc converter [20]. In case of the PSM FB dc–dc converters, the voltage stresses of all power switches are clamped to the input voltage. Thus, high-voltage switching devices such as 600-V switches should be used for the primary side power switches. In case of the proposed converter, S1 and S2 are clamped to Vd while S3 and S4 are clamped to the sum of Vd and Vc . The proposed converter can reduce the voltage stress of power switches. Fig. 5 shows the relation between the duty ratio D and voltage stresses of S3 and S4according to different input voltage conditions. Switch voltage stresses of S3 and S4 can be lower than Vd when D is below0.5. It is beneficial in two-stage applications like EV on-board battery chargers because the use of popular high-performance500–600 V power switches is clearly ensured. From (8) and (9), the voltage across the clamping capacitor can be expressed as

$$V_c = \frac{2D - 1}{N} V_b.$$

Fig. 6 shows the graph for the relation between the duty ratio and the clamping capacitor voltage. It can be positive or negative by the duty ratio. The EV battery pack voltage typically ranges from250 to 450 V for the output voltage of the battery charger [16].Thus, the maximum clamping.

capacitor ivoltage ican ibe idecided iby ithe iallowable ibattery ivoltage irange iand iits icorresponding iduty iratio. iPower iswitches iare iturned iON iat izero ivoltage iat iModes i1 iand4. iFrom iMode i1, ithe ifollowing irelation iis iobtained: i

$$i_{Lm}(t_1) = i_{Lm}(t_0) + \frac{V_d}{L_m} D T_s.$$

Supposed that the proposed converter is lossless with a unity efficiency, the average value of the magnetizing inductor current iLm can be represented as follows:

$$\frac{i_{Lm}(t_1) + i_{Lm}(t_0)}{2} = N i_b$$

where ib is the battery current. From (10) and (11),

$$i_{Lm}(t_0) = N i_b + \frac{V_d}{2L_m} D T_s$$

ZVS of S2 and S3 is naturally achieved by the energy stored in Lm. Meanwhile, ZVS of S1 and S4 can be achieved when the energy stored in Lm is larger than the energy stored in CS1 through CS4 . To achieve ZVS of S1

$$\frac{1}{2} L_m i_{Lm}^2(t_0) > \frac{1}{2}(C_{S1} + C_{S3}) V_d^2 + \frac{1}{2}(C_{S2} + C_{S4})(V_d + V_c)^2$$

B. ZCS Condition

All output diodes are naturally turned ON at zero current at Modes 1 and 4. The diode currents iDo1 and iDo2 should be zer0before Do1 and Do2 are turned OFF. The half-resonant period of the series resonance during Modes 1 and 4 should be finished before each output diode is turned OFF. The following condition should be satisfied for ZCS of output diodes as follows:

$$\sin[\omega_c D_{\max} T_s] = 0, \quad \text{if } D_{\max} \le 0.5$$

$$\sin[\omega_c (1 - D_{\max}) T_s] = 0, \quad \text{if } D_{\max} > 0.5$$

where Dmax is the maximum duty ratio. ωc is the critical angular resonant frequency as ωc = 2πfc . fc is the critical resonant frequency of the series-resonant circuit. For zero-current turn-off of output diodes, the resonant frequency fr should be higher than the critical resonant frequency fc . Then, the resonant capacitor Cr should be determined as follows:

$$C_r < \frac{1}{\omega_c^2 L_{lk}} = \frac{D_{\max}^2 T_s^2}{\pi^2 L_{lk}}, \quad \text{if } D_{\max} \le 0.5$$

$$= \frac{(1 - D_{\max})^2 T_s^2}{\pi^2 L_{lk}}, \quad \text{if } D_{\max} > 0.5.$$

C. Charger System

The charging time and lifetime of the battery have a strong dependency on the characteristics of the battery charger [18]-[20].

Several manufacturers are working worldwide on the development of various types of battery modules for electric and hybrid vehicles. However, the performance of battery modules depends not only on the design of modules, but also on how the modules are used and charged. In this sense, battery chargers play a critical role in the evolution of this technology.

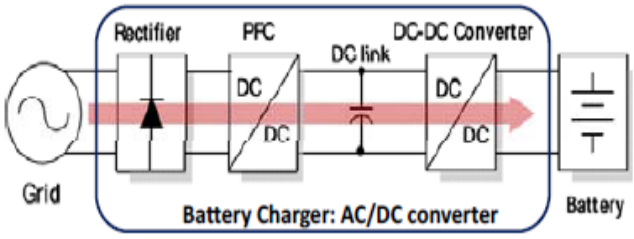

Fig.7 Battery charger system

The conventional battery charger system is shown in Fig. .6 [44]. Because batteries have a finite energy capacity, PHEVs and BEVs must be recharged on a periodic basis ,typically by connecting to the power grid. The charging system for these vehicles consists of an AC/DC rectifier to generate a DC voltage from the AC line, followed by a DC/DC converter to generate the DC voltage required by the battery pack. Additionally, advanced charging systems might also communicate with the power grid using power line.

IV. CONTROL STRATAGY

A. Pulse-Width Modulation

Pulse width modulation (PWM) techniques for two level inverters have beeen studied extensively during the past decades many different PWM methods have been developed to achive the following aims. modulation range,reduced switching loss. losser totall hormonics distortion in the specturnof switching waveform easy implementation.less memory space and computation time on implementation in digital process for the proposed work . The two most widly used PWM scheam for multi-level inverters are the carrier PWM technique and space vector based PWM techniques

Pulse width modulation is a method of controlling the output voltage of an inverter. In this method a control signal is compared with a repetitive signal, typical a triangular signal. To make the converter work in an inverter mode the control signal should have a sinusoidal shape. This control signal can vary a bit and this will be discussed in [13]. At a constant switching frequency the time period of the triangular signal is also constant since this signal gives the switching frequency. This is given in equation (2.1).

$$f_{sw} = \frac{1}{T_{tri}} \quad (3.1)$$

The frequency of the control signal gives the frequency of the desired fundamental output voltage. For a two-level converter there are two switches in one bridge leg and the upper switch will be on when the control signal is greater than the triangular signal. If uni polar switching is chosen the lower switch will be off when the upper is on, which means that it will be off when the control signal is greater than the triangular signal. Switch number 2 will be on when the control signal is lower than the triangular and hence the upper switch will be off. This is shown in the figure below.

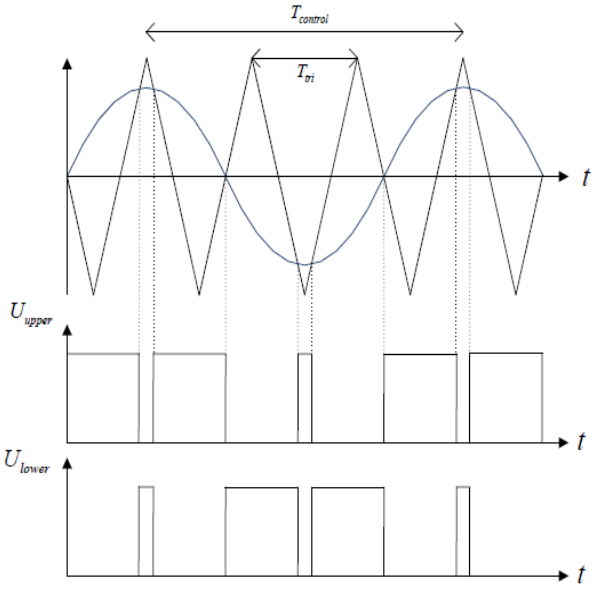

Fig 8: PWM with bipolar switching pattern As it will be seen in the next subchapters the control is a bit more complicated when a three level converter is being used. More about two-level converter control is to be found . There are a few parameters that need to be defined when PWM is discussed.

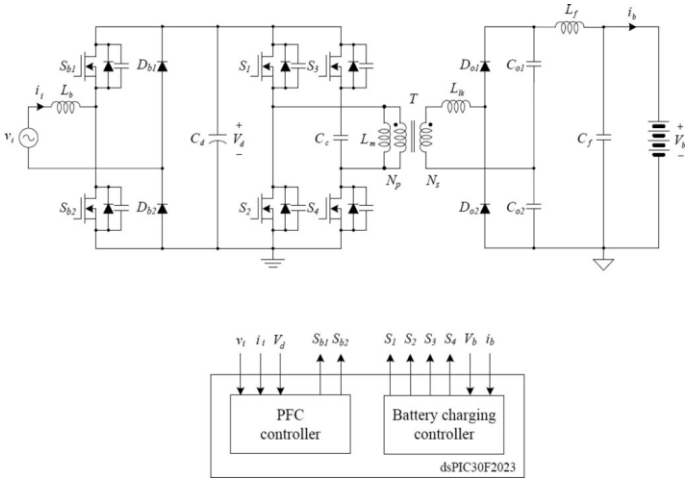

Fig.9. Circuit diagram of the over all system.

V. SIMULATION RESULTS

A2.0-kW prototype circuit of the proposed converter has been designed with a PFC converter. Fig. 9 shows the circuit diagram of the overall system. The bridgeless boost rectifier [23], [24] has been used for the PFC converter. It generates the dc-link voltage V_d around 380–400Vfrom 60Hz/230 Vrms grid voltage.

Published By:
Blue Eyes Intelligence Engineering
and Sciences Publication

The proposed dc–dc converter charges the battery pack with in the output voltage range from 250 to 450 V. The key circuit parameters of the proposed dc–dc converter are as follows

- Switch output capacitor CS : 500 pF;
- Clamping capacitor Cc: 1 μF;
- Transformer turns ratio N: 0.5
- Magnetizing inductor Lm: 100 μH;
- Leakage inductor Llk: 3.5 μH;
- Resonant capacitor Cr: 1 μF;
- output filter inductor Lf : 30 μH;
- output filter capacitor Cf : 20 μF.

Fig. 7 shows the photograph of the designed prototype system. The hardware circuit of the prototype system is divided into two parts: the microcontroller-based control circuit and power circuit. S1 = S2 = S3 = S4 = FCH76N60NF and Do1 = Do2 = HFA50PA60C are used for switching devices. Power switches operate at a constant switching frequency of50 kHz with a dead time of 330 ns. The transformer T is designed by using the ferrite core EE 7066. The transformer has the primary winding turns of Np = 20 and secondary winding turns of Ns = 10. Llk = 3.5 μH and Cr = 1 μF are used for fr = 60 kHz so that the output diode current should be in DCM .Fig. 8 shows the Matlab Simulation waveforms of the proposed dc–dc converter for 2.0 kW. when the output diode current is in the DCM. Fig. 7(a) shows the gating signals vgs1 and vgs2 , primary current ip , and switch voltages VS1 and VS2 when the battery voltage is regulated as Vb = 350 V. The duty ratio D is 0.45. Before the gating signals are applied to S1 and S2 , switch voltages VS1 and VS2 are zero, respectively. ZVS of S1 and S2 is achieved. Switch voltages VS1 and VS2 are clamped to input voltage of 380 V. It is observed that the resonant frequency fr is 60 kHz for Llk = 3.5 μH and Cr = 1 μF. Because the output diode current is in the DCM, the circulating current in the primary side exists.. Fig. 10 shows the Matlab Simulation waveforms of the proposed dc–dc converter for 2.0 kW when the output diode current is in the CCM. It shows the gating signals vgs1 and vgs2, primary current ip , and switch voltages VS1 and VS2 when the battery voltage is regulated as Vb = 350 V. For the CCM operation of the output diode current, the resonant capacitor Cr = 2.2 μF is used with Llk = 3.5 μH. The resonant frequency fr is close to 40 kHz. Because the output diode current is in the CCM , no circulating current occurs, minimizing conduction losses in the primary side. Fig 11 shows the Matlab Simulation waveforms of the proposed dc–dc converter at light-load condition. Fig. 10(a) shows vgs1, vgs2, ip, VS1 , and VS2 for 50 W. Fig. 10(b) shows vgs3, vgs4, Vc, VS3 , and VS4 for 50 W. Before the gating signals are applied to power switches, switch voltages are zero. ZVS of power switches is achieved from light-load to full-load conditions .Fig. 14 shows the Matlab Simulation waveforms when the battery charging controller is applied to the proposed converter .The proposed converter has been tested to charge Li-ion batteries.

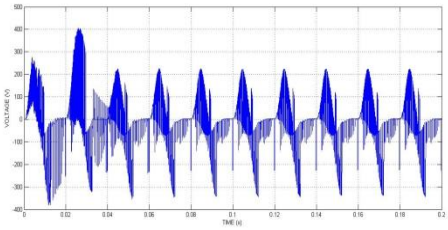

Fig.10. Simulation waveforms of the proposed dc–dc converter for Transformer Primary Voltage.

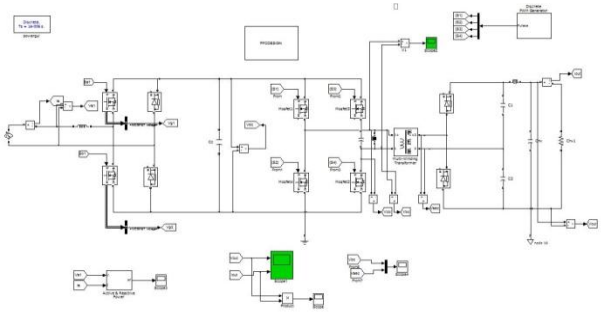

Fig.11. Simulation diagram of proposed model

Fig. 14(a) shows the battery voltage Vb and battery current ib when the proposed converter operates at a cons tant current mode. When the battery power changes from 1.6 to 1.3 kW ,the battery current is constantly regulated as ib = 4 A as the battery voltage Vb changes from 400 to 325 V. Fig. 14(b) shows the battery voltage Vb and battery current ib when the proposed converter operates at a constant voltage mode. When the battery power changes from 0.8 to 1.6 kW, the battery voltage is constantly regulated as Vb = 400 V as the battery current ib changes from2 to 4 A

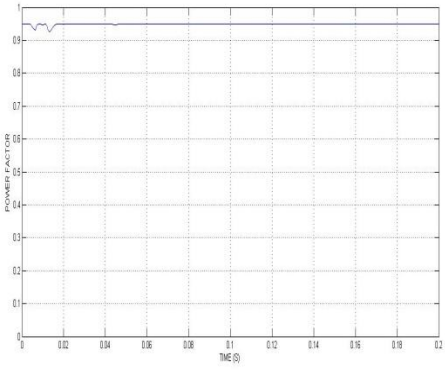

Fig. 12. Simulation waveforms of the proposed dc–dc converter for Power Factor(P.F).

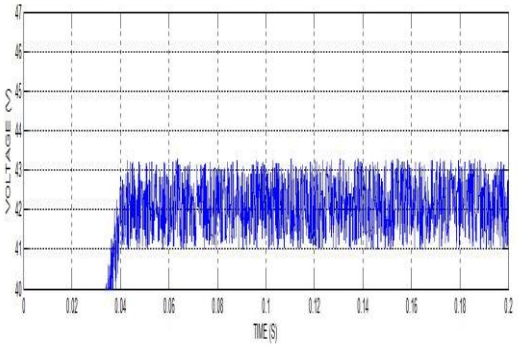

Fig.13 Simulation waveforms of the existing dc–dc converter voltage ripple content

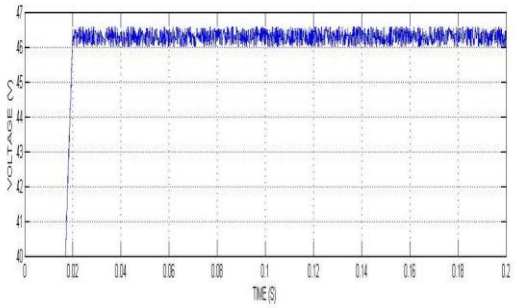

Fig.14 Simulation waveforms of the proposed dc–dc converter voltage ripple content

in this proposed converter will reduce voltage ripple in 2V and improve the voltage level in standard voltage

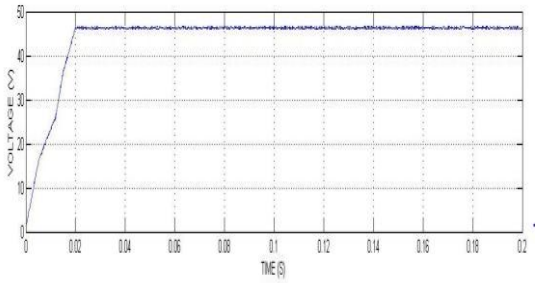

Fig. 15. Simulation waveforms of the proposed dc–dc converter for Output Voltage (Vout).

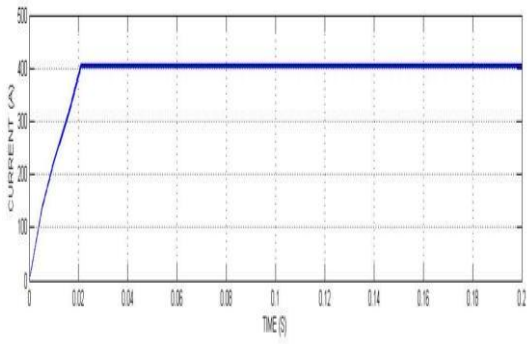

Fig. 17. Simulation waveforms of the proposed dc–dc converter for Output Current (Iout).

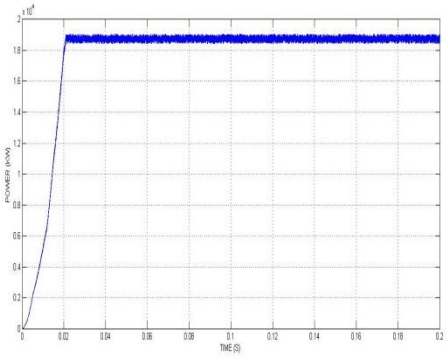

Fig. 19. Simulation waveforms of the proposed dc–dc converter for Output Power (Pout).

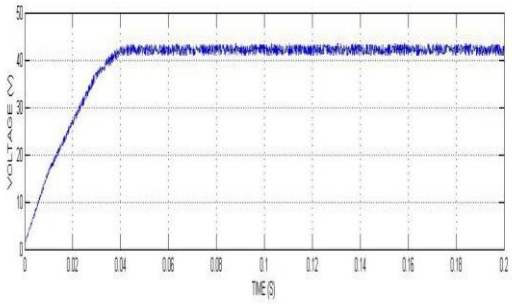

Fig. 16. Simulation waveforms of the existing dc–dc converter for Output Voltage (Vout).

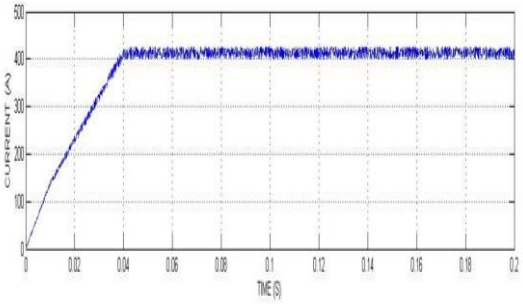

Fig. 18. Simulation waveforms of the existing dc–dc converter for Output Current (Iout).

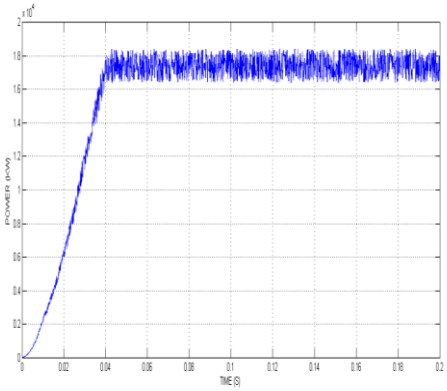

Fig. 20. Simulation waveforms of the existing dc–dc converter for Output Power (Pout).

VI. CONCLUSION

This paper has proposed a high-efficiency soft-switching PWM dc–dc converter for high-frequency-link battery chargers. ZVS of power switches is achieved by using a complementary PWM. Wide range soft-switching operation is achieved without using any additional switching circuits. Furthermore, ZCS of output diodes is achieved by effectively using a series resonance between the transformer leakage inductor and secondary side rectifier circuit components. Reverse-recovery losses of output diodes are eliminated without using any additional circuit components. It has been investigated that the circulating current in the primary side can be changed by the operation modes of the output diode current. The converter control strategy has been suggested, including its digital implementation .The performance of the proposed converter has been verified throughout Matlab simulation results for a 2.0-kW prototype circuit. Matlab simulation results confirm that the proposed converter improves the power efficiency compared to the previous converters. The proposed converter achieves a peak efficiency of 98.3% at 15 kW and a high-efficiency of 98.0% at 19 kW. .

REFERENCES

1. M.Yilmaz iand iP. iT.Krein, i“Reviewof ibattery icharger itopologies, ichargingpower ilevels, iand iinfrastructure ifor plug-in ielectric iand ihybrid ivehicles,”IEEE iTrans. iPower iElectron., ivol. i28, ino. i5, ipp. i2151–2169, iMay i2013. i
2. M. iPahlevaninezhad, iP. iDas, iJ. iDrobnik, iP. iK. iJain, iand iA. iBakhshai, i“AZVS iinterleaved iboost iac/dc iconverter iused iin iplug-in ielectric ivehicles,”IEEE iTrans. iPower iElectron., ivol. i27, ino. i8, ipp. i3513–3529, iAug. i2012. i
3. M. iPahlevaninezhad, iP. iDas, iJ. iDrobnik, iP. iK. iJain, iand iA. iBakhshai, i“Anovel iZVZCS ifull-bridge idc/dc iconverter iused ifor ielectric ivehicles,” iIEEETrans. iPower iElectron., ivol. i27, ino. i6, ipp. i2752–2769, iJun. i2012. i
4. C. iY. iOh, iD. iH. iKim, iD. iG. iWoo, iW. iY. iSung, iY. iS. iKim, iand iB. iK. iLee,“A ihigh-efficient inonisolated isingle-phase ion-board ibattery icharger iforelectric ivehicles,” iIEEE iTrans. Power iElectron., ivol. i28, ino. i12, ipp. i5746–5757, iDec. i2013. i
5. D. iS. iGautam, iF. iMusavi, iM. iEdington, iW. iEberle, iand iW. G. iDunford,“An iautomotive ionboard i3.3-kW ibattery ichargers ifor iPHEV iapplication,”IEEE iTrans. iVeh. iTechnol., ivol. i61, ino. i8, ipp. i3466–3474, iOct. i2012. i
6. T. iMishima, iK. iAkamatsu, iand iMutsuo iNakaoka, i“A ihigh ifrequencylinksecondary-side iphase-shifted ifull-range isoft-switching iPWM idc–dcconverter iwith iZCS iactive irectifier ifor iEV ibattery ichargers,” iIEEE iTrans.Power iElectron., ivol. i28, ino. i12, ipp. i5758–5773, iDec. i2013. i
7. D. iS. iGautam, iF. iMusavi,W. iEberle, iandW. iG. iDunford, i“A izero-voltageswitching ifull-bridge idc–dc iconverter iwith icapacitive ioutput ifilter ifor ipluginhybrid ielectric ivehicle ibattery icharging,” iIEEE iTrans. iPower iElectron.,vol. i28, ino. i12, ipp. i5728–5735, iDec. i2013. i
8. R. iRedl, iN. iO. iSokal, iand iL. iBalogh, i“A inovel isoft-switching ifull-bridgedc/dc iconverter: iAnalysis, idesign iconsiderations, iand iMatlab iSimulation iresultsat i1.5 ikW, i100 ikHz,” iIEEE iTrans. iPower iElectron., ivol. i6, ino. i3, ipp. i408–418, iJul. i1991. i
9. W. iChen, iX. iRuan, iand iR. iZhang, i“A inovel izero-voltage-switching iPWMfull ibridge iconverter,” iIEEE iTrans. iPower iElectron., ivol. i23, ino. i2,pp. i793–801, iMar. i2008. i
10. W. iChen,X.Ruan, iQ. iChen, iand iJ. iGe, i“Zero-voltage-switching iPWMfullbridgeconverter iemploying iauxiliary itransformer ito ireset ithe iclampingdiode icurrent,” iIEEE iTrans. iPower iElectron., ivol. i25, ino. i5, ipp. i1149–1162, iMar. i2010. i
11. Y. iD. iKim, iK. iM. iCho, iD. iY. iKim, iand iG. iW. iMoon, i“A inew iphaseshiftedfull-bridge iconverter iwith imaximum iduty ioperation ifor iserverpower isystem,” iIEEE iTrans. iPower iElectron., ivol. i26, ino. i12, ipp. i3491–3500,iDec.i2011

AUTHORS PROFILE

Mr.Meenavalli Harikrishna
Graduated from Aditya College of Engineering, Surampalem. He is presently pursuing M.Tech in the Department of Electrical and Electronics Engineering, Pragati Engineering College,Surampalem, Peddapuram. His research areas include Power Electronics Converters, Drives, Renewable energy systems, and storage systems. meenavalliharikrishna@gmail.com

Mr.Madugula Satya Harish, Post Graduated from University college of Engineering , Vizianagaram. He is presently working as Assistant Professor in the Department of Electrical and Electronics Engineering, Pragati Engineering College, Surampalem, Peddapuram. He had published 2 research papers in Inter National journals. His research area is Power Systems. he has an IAENG ,CSTA, JETIR membership. harish6172@gmail.com.

Mr.M.V.Chandra Kumar, Post Graduated from JNTUK University, He is presently working as Assistant Professor in the Department of Electrical and Electronics Engineering, Pragati Engineering College, Surampalem He had published 2 research papers in Inter National journals. 0